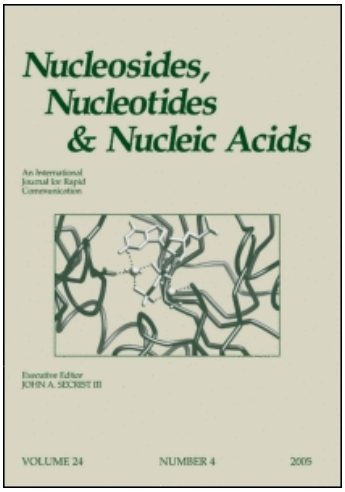

Nucleosides, Nucleotides and Nucleic Acids
Publication details, including instructions for authors and subscription information:
http://www.informaworld.com/smpp/title~content=t713597286

Conformation and Local Environment of Nucleotides Bound To Hiv Type 1 Reverse Transcriptase (HIV-1 RT) in The Ground State

George R. Painter[a]; C. Webster Andrews[b]; Phillip A. Furman[a]
[a] Triangle Pharmaceuticals, Inc., Durham, NC, USA [b] Glaxo Wellcome Inc., Research Triangle Park, NC, USA

To cite this Article Painter, George R. , Andrews, C. Webster and Furman, Phillip A.(2000) 'Conformation and Local Environment of Nucleotides Bound To Hiv Type 1 Reverse Transcriptase (HIV-1 RT) in The Ground State', Nucleosides, Nucleotides and Nucleic Acids, 19: 1, 13 — 29
To link to this Article: DOI: 10.1080/15257770008032994
URL: http://dx.doi.org/10.1080/15257770008032994

NUCLEOSIDES, NUCLEOTIDES & NUCLEIC ACIDS, 19(1&2), 13–29 (2000)

CONFORMATION AND LOCAL ENVIRONMENT OF NUCLEOTIDES BOUND TO HIV TYPE 1 REVERSE TRANSCRIPTASE (HIV-1 RT) IN THE GROUND STATE

George R. Painter *[a], C. Webster Andrews [b] and Phillip A. Furman [a]

[a]Triangle Pharmaceuticals, Inc. Durham, NC (USA), [b] Glaxo Wellcome Inc., Research Triangle Park, NC (USA)

Dedicated to the memory of Dr. Gertrude B. Elion

ABSTRACT: Nuclear Overhauser effect experiments were used to characterize the protein environment and conformations of dTTP, dATP and AZTTP bound to HIV-RT in the ground state. The results show the initial binding sites for the nucleotides overlap but are not completely coincident. All of the bound nucleotides assume the same anti C4'-exo conformation.

INTRODUCTION

The Mg^{2+}-dependent human immunodeficiency virus type I (HIV-1) reverse transcriptase (EC 2.7.7.49, RT) catalyzes the transcription of HIV-1 genomic RNA to double-stranded DNA via RNA- and DNA-directed DNA synthesis. The 117-kDa-enzyme complex isolated from intact virions is a dimer of two polypeptides of molecular weights 66,000 and 51,000 [1,2]. The 66 kDa subunit has polymerase and RNAse H activity [3]. Like other retroviral reverse transcriptases, the RNAse H domain is located in the carboxy terminal portion of the polypeptide. The 51 kDa subunit is derived from the 66 kDa polypeptide by cleavage at a protease- sensitive site on the link between the polymerase and RNAse H domains [4].

DNA synthesis by heterodimeric HIV-1 RT occurs via a bireactant/biproduct reaction mechanism similar to that proposed for several other DNA polymerases [5]. In this mechanism, binding of the reactants is ordered; template-primer binding occurs first,

followed by the binding of a 2'-deoxynucleoside- 5'-triphosphate (dNTP) substrate [6]. If the dNTP has Watson-Crick complementarity to the next appropriate template residue, then the ternary, ground-state complex isomerizes to the Michaelis complex. The nucleoside-5'-monophosphate is then incorporated into the nascent chain via an SN_2 displacement of pyrophosphate from the dNTP by the 3' hydroxyl at the primer terminus [7].

Several structures of HIV-RT either unliganded or complexed with an NNRTI or primer/template have been published [8,9]. The structure of RT with a bound primer/template shows that the primer terminus lies near the three aspartic acid residues required for catalysis and that the double strand extends along the enzyme to the RNAse H domain in a deep cleft. Although these structures have provided valuable insight into the structure/function of the RT, they have provided little information regarding the topography of the dNTP binding site and the structural features of the interaction of nucleotide analogues with this site. Recently, Huang et al. [10], using a thiol-tethered primer/template and RT with a glutamine to cysteine change at position 258, formed a stalled complex of RT, primer/template, and a nucleoside 5'-triphosphate (AZTTP). A crystal structure of this complex, at 3.2 Å resolution, showed that formation of the catalytic complex involves a significant conformational change. In the catalytic complex there is a well-defined binding site for substrates, including a pocket that accommodates the 3'-OH of dNTP's and the 3'-azido group of AZTTP. Based on this study insight into the mechanism of polymerization and the role of specific amino acids or clusters of amino acids in substrate utilization during the polymerization process has been gained.

Here we report the use of nOes to probe the protein environment of two nucleotides, dATP and dTTP, and the nucleotide analogue AZTTP when bound to HIV-RT in the ground state (before the conformational change to form the catalytic complex) and to examine the conformation of the ligand in the bound state. The object is to begin to examine the nature of this initial recognition site(s) since it might provide an additional point at which the enzyme could be competitively inhibited.

MATERIALS AND METHODS

Materials. dATP and dTTP were obtained from Pharmacia. The 5'triphosphate of AZT (AZTTP) was synthesized according to published procedures. The purity of the 5'-triphosphates was established by ^{1}H and ^{31}P NMR, ion exchange chromatography, and TLC [11]. TRIS-d (Merck, Sharp, and Dohme), 99% $^{2}H_20$ (Aldrich), ultrapure KCl and $MgCl_2$

(Fischer Chemicals) were purchased and used without further purification. HIV-1 RT was expressed in E. coli TG-1 from the recombinant plasmid pRT1 and was isolated using a modification of the method of Tisdale et al. [12] in which anion exchange chromatography with Q-Sepharose (Sigma) was substituted for the affinity chromatography step. Enzyme purity, monitored by SDS-PAGE, was greater than 90%, and two bands of approximately equal molar proportions corresponding to p66 and p51 were observed. The activity of the purified enzyme was assayed by the DEAE-filter paper-binding assay using poly(rA)$_{50}$-oligo (dT)$_{10}$ as template primer and [^{3}H]-dTTP as substrate [13]. Protein NMR samples were treated with Chelex 100 (Biorad) before use to remove any cationic, paramagnetic impurities; concentrated to the appropriate volume with an Amicon centricon-10 concentrator; and dialyzed against five changes of standard buffer (10 mM TRIS-d, 100 mM KCl, pD 7.6 in $^2H_20$) at 4 °C. Protein concentrations were determined spectrophotometrically using an extinction coefficient of 333,450 $M^{-1}cm^{-1}$ at 279 nm [14].

NMR spectroscopy. Proton NMR spectra were recorded at an observation frequency of 499.843 MHz on a Varian VXR-500S spectrometer. Typical NMR samples contained 76 μM HIV-1 RT in standard buffer, 2 mM $MgCl_2$, and varying concentrations of dTTP, AZTTP, or dATP ranging from 0 to 2.0 mM. The ligand in the sample was added from a stock solution, the concentration of which was determined spectrophotometrically using published extinction coefficients [15]. All measurements were made at 25 °C. Chemical shifts were expressed relative to external sodium 2, 2-dimethyl-2-silapentane-5-sulfonate (DSS). The nOe difference spectra were obtained with an interleaved pulse sequence previously described in detail in the literature [16]. A decoupler irradiation power of 12 μW was chosen to produce complete saturation at ω_1 with the shortest t_1 used, 100 ms. The magnitudes of the nOes were determined by integration and by gravimetric analysis as described by Glasel [17].

NMR Data Analysis. Under the condition of fast, reversible binding, the apparent K_d value for ligand binding to protein can be obtained by fitting ligand line widths at half intensity, Δv_{obs}, to equation 1:

$$1/\Delta v_{obs}=(1/\Delta v_f - 1/\Delta v_b)[dNTP]_t/(K_d + [dNTP]_t) + 1/\Delta v_b \qquad \{1\}$$

where $[dNTP]_t$ is the total ligand concentration, Δv_f is the line width of free dNTP, and Δv_b is the line width of bound dNTP [18]. The stoichiometry of dTTP binding can be established

from a linear version of the Hill equation:

$$\log (\Delta v_f/(\Delta v_{obs} - \Delta v_f) = n\log[dNTP] - \log (K') \qquad \{2\}$$

where n is the order of the binding reaction with respect to ligand concentration and K' is the concentration of ligand that yields 50% of $1/\Delta v_f$ [19].

The theoretical and experimental aspects of the use of truncated driven nOe (TOE) experiments to establish the conformation of a protein-bound ligand (in a two-site ligand-protein exchange equilibrium) have been discussed extensively [20-23]. Given the condition of fast exchange of the ligand on and off the binding site relative to the spin-lattice relaxation and cross-relaxation rates, the initial build-up rate of the TOE to spin i upon irradiation of spin j can now be quantitated using equation 3:

$$dI_z/dT_{t=0} = -f_B\sigma^B_{ij} - (1-f_B)\sigma^F_{ij} \qquad \{3\}$$

where f_B is the fraction of bound nucleotide σ^B is the cross-relaxation rate in the bound state and σ^F is the cross-relaxation rate in the free state [23]. The increased rotational correlation time, τ_c, of the bound ligand relative to the free ligand results in the inequality $f_B\sigma^B_{ij} >> (1-f_B)\sigma^F_{ij}$, which simplifies the initial build-up rate in equation 3 to $-f_B\sigma^B_{ij}$. The dominance of σ^B_{ij} in the cross -relaxation term is confirmed experimentally by the observation of negative nOes between the ligand proton pairs in the presence of protein. Bound ligand distance ratios can be calculated from TOE experiments by determining the initial build up rates of nOes of ligand resonances, or from pre-steady-state nOes determined using equation 4:

$$r_{ij}/r_{ik} = (\sigma^B_{ik}/\sigma^B_{ij})^{1/6} = (\eta_{ik}/\eta_{ij})^{1/6} \qquad \{4\}$$

where r_{ij} is the distance between protons i and j, r_{ik} is the distance between protons i and k, η_{ij} is the nOe between protons i and k upon irradiation of k, and η_{ij} is the nOe between protons i and j upon irradiation of j [24]. Use of the nOe ratio method described by equation 4 requires two interproton distances with a proton in common, resulting in cancellation of cross-relaxation terms.

Theoretical fits to the observed nOe build up rates described by equation 4 were obtained with the use of a second-order polynomial [17]. The initial slope can be used to distinguish primary nOes from secondary nOes, since primary nOes increase linearly with

increasing values of t_1 at short irradiation times while secondary nOes display an initial lag in buildup rate due to transfer of magnetization from the initial spin to a second spin.

Molecular Modeling. Molecular mechanics was used to model the conformational equilibria of the nucleotides and to establish the effects of the glycosidic angle (χ), the exocyclic C4'-C5' dihedral angle (γ), and the pseudorotational phase angle (P) on interproton distances (r). Models were built using MacroModel [25] and the AMBER force field of Weiner et al. [26], modified by addition of parameters necessary for the azide group in AZT. The detailed derivation of these parameters has been reported previously [27]. Equilibrium bond length and valence angles were obtained from the X-ray crystallographic structure of AZT [28]. Torsional constants for the two C-C-N-N dihedral angles were derived using the model compound ethyl azide [27]. Charges for the 3'-azido-2',3'-dideoxyribosyl fragment of AZTTP were determined using the electrostatic potential fit method, and standard AMBER charges were used for the thymine ring. The charges of the C1' and N1 atoms were scaled so that the overall molecular charge was zero. This formulation of charges for the molecule is consistent with the methodology used in deriving charges for the AMBER database [29]. The VDW parameters for the azide nitrogens were those suggested by Herzyk et al. [30]. The new parameters were inserted into the all-atom AMBER force field. Minimization with constraints was used to set the ring pucker of the 2'-deoxy- and 3'azido-2',3'-dideoxyribose rings. Minimizations were carried out in two stages using the steepest descent algorithm for 50 iterations followed by the conjugate gradient method until convergence was complete. A distance-dependent dielectric was used. P was then computed for each minimized structure using torsional angles generated with the equation published by Hassnoot [31].

RESULTS

Titration of HIV-1 RT with ligand. The 500 MHz ^{1}H NMR spectrum of free HIV-1 RT (Figure 1a) consists of a series of broad, overlapping resonances typical of a high molecular weight protein with a large τ_c. In contrast, the line widths at half intensity, $\Delta\nu_{obs}$, of the ^{1}H resonances of free dTTP, AZTTP, and dATP are quite narrow as illustrated for the case of dTTP in Figure 1b. The values of $\Delta\nu_{obs}$ increase substantially in the presence of protein (Figure 1c). This increase is probably the result of a decrease in τ_c of the small molecule in the bound state and/or an increase in the number of magnetic neighbors. Figure 2 shows the effect of increasing the ligand-to-RT ratio on the $\Delta\nu_{obs}$ of the H6 resonance of dTTP. As the concentration of ligand is increased, the $\Delta\nu_{obs}$ of H6 decreases until a final ligand: HIV-1 RT

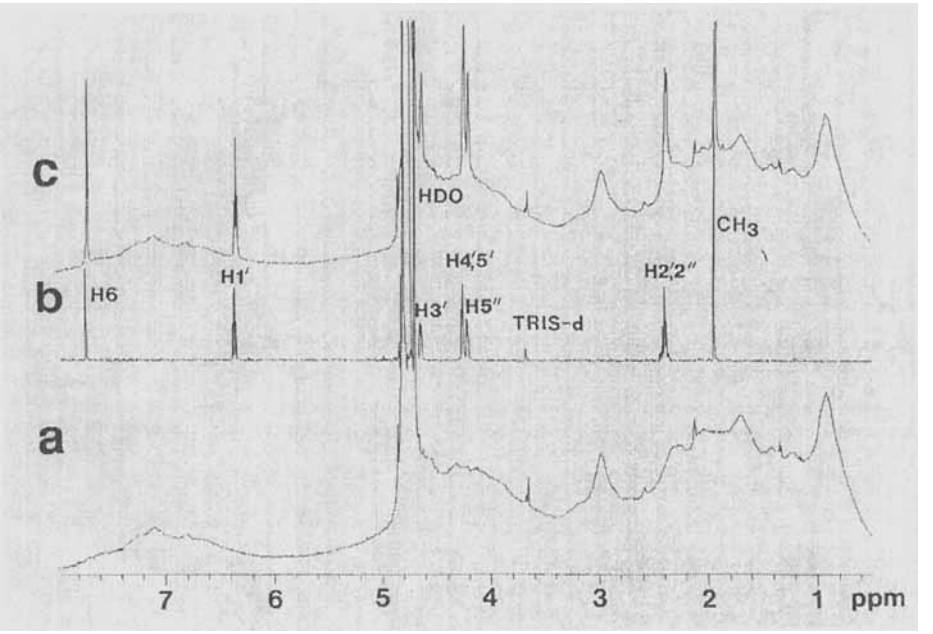

1. 500 MHz ^{1}H NMR spectra of (a) 72 μM HIV-1 RT in standard buffer containing 2 mM $MgCl_2$, (b) 2 mM dTTP in the same buffer, and (c) 72 μM HIV-1 RT in 0.6 ml standard buffer containing 2 mM $MgCl_2$ to which a 5 μl aliquot of 14 mM dTTP had been added. ^{1}H NMR spectra were recorded at 25 °C on a Varian VXR-500S spectrometer with an observation frequency of 499.843 MHz. Acquisition parameters: spectral window, 4800 HZ; data points 32K; 90° pulse (12.5 μs); delay between pulses, 2 sec; 256 accumulations.

ratio of 24 is reached. Addition of more dTTP produces no further change in Δv_{obs}, in accord with the system being in fast exchange between the free and bound form of the ligand. Non-linear least-squares regression analysis of the data in Figure 2 using equation 1 yielded a K_d value of 7.92±1.06 x 10^{-5} M and a Δv_b of 21 Hz. A replot of the data using equation 2 and data points near the 50% saturation point (79 μM) yields a Hill coefficient of 1.04±0.09 (see insert, Figure 2).

This K_d is similar to that calculated using endogenous tryptophan fluorescence [14]. In the fluorescence study, the presence of homopolymeric template-primer did not alter the apparent K_d values for dNTPs. Thus Watson-Crick base pairing does not appear to be involved in initial dNTP binding, but is a key interaction in triggering the conformational change to the catalytic complex. For this reason, nucleic acid template-primers were not added to the protein for the nOe experiments described here. Similar observations of the

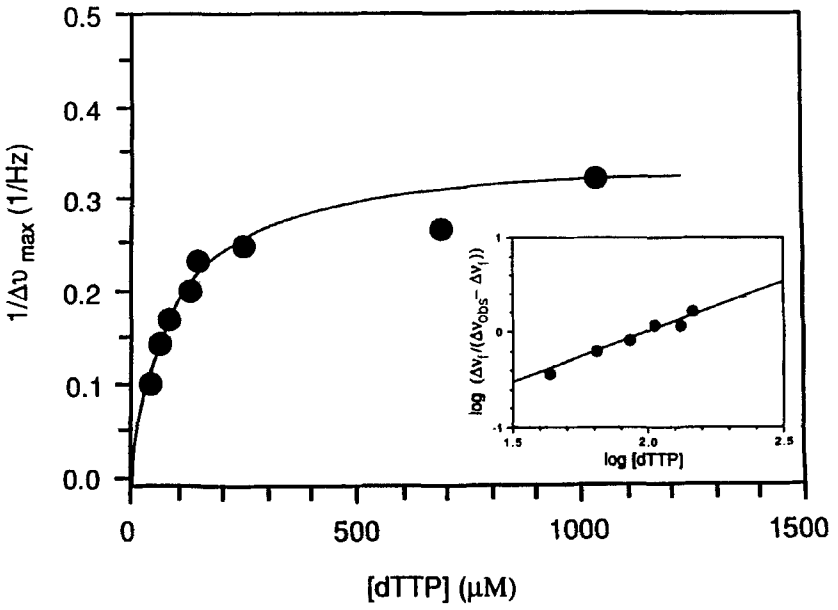

2. The effect of increasing dTTP concentration on the $1/\Delta\nu_{obs}$ of the H6 resonance of dTTP. Aliquots of a stock 14 mM dTTP solution were added to the 76 μM buffered enzyme sample, mixed by inversion, and the spectrum acquired after 10 min. using the acquisition parameters described in the legend of Figure 1. The line represents the fit of the data to equation 1. The line shown in the insert is the fit of the replotted data to equation 2.

noninvolvement of nucleic acid in initial dNTP binding have been made in NMR studies of dTTP bound to the Klenow fragment of DNA polymerase I [11] and in a preliminary NMR study of ddATP bound to HIV-1 RT [32].

Intermolecular nOes from HIV-1 RT to Bound Nucleotide. The environment of the protein-bound nucleotides was probed using nOe differences spectroscopy experiments. Protein resonances were irradiated for 0.4 s and nOes to dTTP, dATP, and AZTTP were monitored. This t_1 produced maximal transferred nOe but minimal spin diffusion (*vida infra*). The observed nOes are negative; indicating the relaxation of the nucleotide is modulated by the large τ_c of the protein. At the operative signal-to-noise ratio of 210:1, nOes greater than 0.5% were considered above background. The nOe action spectra of the protein aromatic region of the dTTP-, AZTTP-, and dATP-complexes were obtained by irradiating the protein resonances between 6.6 and 7.4 ppm at 20 Hz intervals and monitoring the magnitude of the nucleotide nOes. Selective nOes between ligand and protein aromatic resonances were only observed in the dATP and dTTP complexes (Table 1). Irradiation between 6.71 and 6.75

TABLE 1. Transferred nOes to a dNTP observed upon irradiation of HIV-1 RT resonances. The value of the nOes were obtained using double resonance difference spectroscopy and an irradiation time of 0.4 s at the indicated frequency ω_1. The error is approximately ± 10% for nOes with magnitudes > 6 % and ± 25% for nOes of lower magnitude.

ω_1[a]	dNTP	'H Resonance (-% nOe)				
7.20±0.02	dTTP	H'1(5.7)	H2'/H2" (25.0)[b]	H6(3.5)		
7.00±0.02	dATP	H1'(3,0)	H2'(2.4)	H2"(13)		
6.73±0.02	dTTP	H1'(3.4)	H2'/H2"(2.3)			
	dATP	H1'(5.5)	H2'(11)	H2"(3.0)	H8(2.2)	
1.65±0.02	AZTTP	H1'(3.4)	H2'/H2"(5.6)[b]	CH_3(8.5)		
	dTTP	H1'(2.2)	CH_3(4.1)			
1.34±0.02	dATP	H2"(4.0)	H8(2.5)			
1.26±0.02	AZTTP	H5'/H5" (3.3)[c]				
	dTTP	H1"(1.6)	H6(1.4)	CH_3(2.0)		
	dATP	H1'(2.6)	H2'(4.0)	H5'/H5"(4.0)	H2(4.2)	
1.02±0.02	AZTTP	H1'(3.0)	H2'/H2"(3.0)			
	dTTP	H1'(3.2)	CH_3(2.5)			
0.97±0.02	dATP	H1'(4.0)	H2'(4.0)	H5'/H5"(2.7)[c]	H8(4.2)	H2(6.3)
0.79±0.02	AZTTP	H1'(3.0)	H2'/H2"(4.0)	CH_3(2.0)		
	dTTP	H1'(2.7)	CH_3(2.3)			
	dATP	H1'(3.8)	H5'/H5"(5.3)[c]	H8(3.0)	H2(7.3)	
0.69±0.02	AZTTP	H2'/H2"(4.0)				
	dTTP	H2'/H2"(2.0)	H6(3.0)	CH_3(3.0)		

TABLE 1 Continued

0.58±0.02	AZTTP	H1'(3.0)
	dTTP	H6(3.0)
	dATP	H8(2.0)

a ω_I is the irradiation frequency in ppm that produced the maximal nOe

b H2'/H2" resonances overlap

c H5'/H5" resonances overlap

ppm produced nOes to the HI' and H2'/H2" resonances of dATP and dTTP, and to the H8 resonance of dATP. nOes exclusive to the 2'-deoxyribose moiety of dATP were observed upon irradiation at 7.00 ppm, and nOes exclusive to dTTP were produced upon irradiation at 7.20 ppm. Irradiation of the aliphatic protein resonances between 0.50 and 2.80 ppm at 20 Hz intervals yielded a complex pattern of transferred nOes to all three ligands with considerable overlap of the nOe action spectra (Table 1). nOes common to all three ligands are observed upon irradiation at 0.58±0.02 ppm, 0.79±0.02 ppm, and 1.26±0.02 ppm. nOes common to the two-pyrimidine nucleotides are observed at w_I values of 0.69±0.01 ppm, 1.02±0.02 ppm and 1.65 ±0.02 ppm. Although irradiation at these frequencies gives rise to nOes common to dTTP and AZTTP, different ligand resonances are also involved (Table 1). nOes exclusive to dATP are observed upon irradiation at 0.97 and 1.34±0.01 ppm.

Nucleotide Intramolecular Nuclear Overhauser Effects and Enzyme bound Nucleotide Conformation. TOE experiments were performed to establish the conformation of the protein-bound nucleotides. Negative intramolecular ligand nOes are observed in the presence of protein in accord with the relaxation rates of the ligand resonances being controlled by the protein τ_c in the bound state (i.e. the dominance of the $f_B\sigma^B_{ij}$ term in equation 3). The magnitude of the TOEs (Table 2) was determined either from nOe buildup curves or from pre-steady state conditions. A typical time-dependence curve for nOe buildup is shown in Fig. 3 for the case of the dATP-RT complex (ligand-to-RT ratio of 40/1). Data in Figure 3 was fit to a second-order polynomial equation to distinguish primary from secondary nOes [17]. In the presence of RT, the nOes observed to the HI' and H8 resonances of dATP upon

TABLE 2. Normalized magnitudes of the TOEs of bound nucleotide. The values of the TOEs were obtained using double resonance difference spectroscopy and an irradiation time of 0.40 s.

Hi	Hj	-%nOe		
		dTTP	AZTTP	dATP
H6	H1'	0.00±0.5	0. 0±0.5	
H6	H2'	6.45±0.60	17.04±1.70	
H6	H3'	0.75±0.19	4.24±1.06	
H6	H5"	1.35±0.34	1.47±037	
H8	H1'			0.0±0.5
H8	H2'			06.96±0.70
H8	H3			1.44±0.36
H8	H5',5"			1.17±0.29
H4'	H1'	0.65±0.16	4.45±1.11	3.18±0.80
H4'	H2"	0.64±0.16	3.43±0.86	2.19±0.55
H3'	H5"	4.00±0.40	a	
H2'	H2"			14.0±2.0

[a]overlap of H4', H5' and H5" resonances

irradiation of the H2' resonance increased linearly with time to approximately 0.6 s, indicating them to be primary. A lag was observed in the build-up rate of the adenine H2 nOe, which may arise from magnetization transfer from the 2'-deoxyribose H2' resonance to the H2" resonance and then to the adenine H2 resonance. The lack of nOes from the ribose H2' resonance to the overlapping H5'/H5" resonances indicates that spin diffusion throughout the entire protein is not a major problem under the experimental conditions employed.

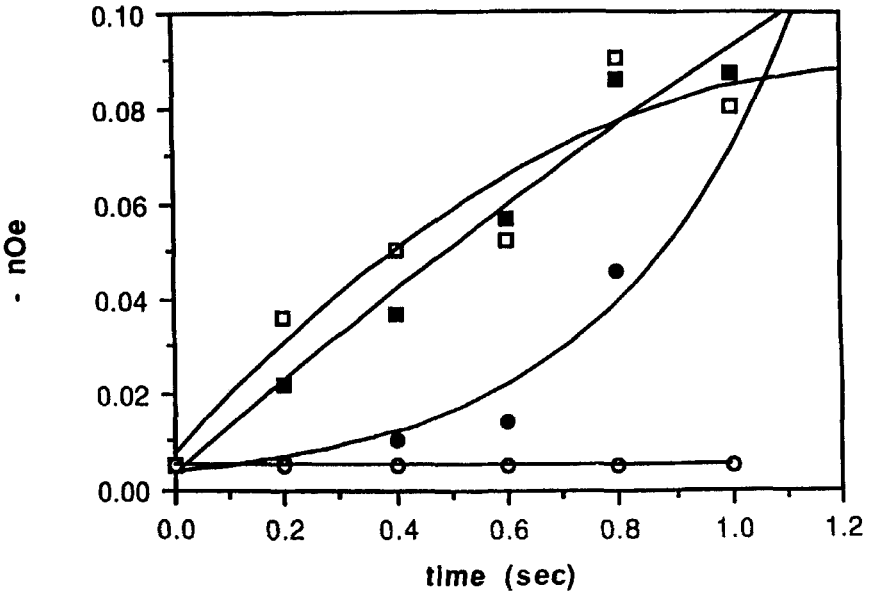

3. The magnitude of intramolecular nOes observed in the dATP-HIV-1 RT complex as a function of the preirradiation time. Representative nOes resulting from irradiation of the dATP H2' resonance are to the H8 (-□-), H2 (-•-) Hl' (-■-) and H5'/H5" (-o-) resonances. The sample contained 76 uM HIV-1 RT, 3.0 mM dATP, and 3.0 $MgCl_2$ in standard buffer. The curves represent the best fit of the data to a second order polynomial quation.

Molecular Modeling of Nucleotide Conformation. A quantitative analysis of nucleotide conformation using the nOe ratio method requires a model that will show the effect of χ (glycosidic angle), P (pseudoratational phase angle of the deoxyribase ring), and γ (C4'-C5'rotational angle) on the values of interproton distances, r_{ij} [27]. In general, two sets of models need to be built for each ligand, one with χ fixed to give a syn conformation and the other with χ fixed to give an anti conformation. The observation of nOes between the H6 and the H2',H3' resonances of dTTP and AZTTP and between the H8 and the H2', H3' resonances of dATP , and the lack of nOes between the Hl' and the H6, H8 resonances (Table 2) indicated that the ligands are exclusively anti in the presence of protein and limited to χ, values between -95^0 to -155^0.γ was fixed +synclinal (+sc) in accordance with previous experimental data [27,33,34] and with the observation of nOes between the H5" and H6 resonances of dTTP and AZTTP and between the H5" and H8 resonances of dATP (Table 2). Further support for the +sc orientation of the C4'-C5' rotor was the observation of a nOe between the H3' and H5" resonances of dTTP. This nOe could not be measured for AZTTP and dATP due to spectral overlap. To scan the pseudorotational phase angle range from 0-

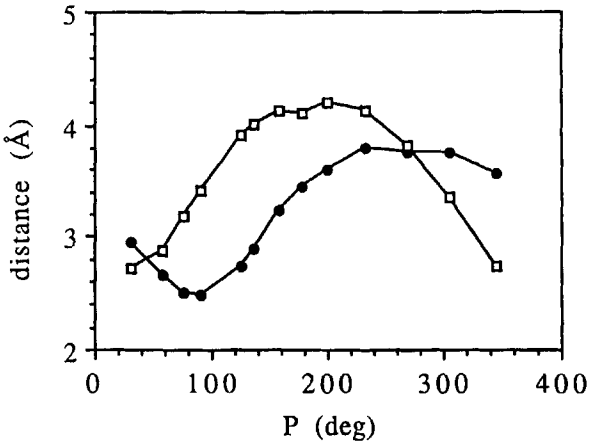

4. Dependence of the interproton distances $r_{4'1''}$ (closed circles) and $r_{4'2'}$ (open squares) on P for the anti conformation of dAZT.

360°, envelope forms of the 2'-deoxyribose and 3'-azido 2', 3'-dideoxyribose rings were built as described in the Methods section. In all cases, the $r_{4'2''}$ and $r_{4'1'}$ values are a function of P (Figure 4) but are independent of small changes in χ. Thus the ratio of these two distances is a good indicator of the conformation of the 2'-deoxyribose and 3'-azido-2'3'-dideoxyribose moieties. The $r_{2'2''}$ value, 1.79 A, did not vary as a function of P and was used as a calibration distance. Because the H2' and H2" resonances of dTTP and AZTTP were partially overlapping, the region was irradiated in 5 Hz intervals to determine selectivity attributable to each resonance. The P values of bound ligands were determined by comparing experimentally-determined ratios of $r_{4'2''}/r_{4'1'}$ (Table 3) with the ratios derived from the curve in Figure 4. The results are given in (Table 3). To obtain a more precise estimate of the χ of the bound ligands, a second set of models was built with P fixed at 55° and 62°, (values consistent with the experimentally determined $r_{4'2''}/r_{4'1'}$ values) and χ fixed +sc. χ was varied in 10° increments through the anti range (-95° to -155°), and the model was minimized with χ constrained after each rotation. The distances $r_{83'}$ (dATP), $r_{82'}$(dATP), $r_{63'}$(dTTP and AZTTP), and $r_{62'}$ (dTTP and AZTTP) varied as a function of χ in all cases. The refined χ values were obtained by comparing the experimentally determined distance ratios, $r_{83'}/r_{82'}$, and $r_{63'}/r_{62'}$, to model-derived values. The optimized values of χ are shown in (Table 3).

TABLE 3. Experimentally determined distance ratios, ring puckering (P), and glycosidic bond torsional angles (χ) of nucleotides bound to HIV-1 RT.

	dTTP	AZTTP	dATP
$r_{63'}/r_{62'}$	1.43±0.08	1.26±0.05	
$r_{4'2'}/r_{4'1'}$	1.00±0.09	1.05±0.09	1.06±0.14
$r_{83'}/r_{82'}$			1.30±0.08
P (degrees)	55±8	60±10	62±10
χ(degrees) [a]	-110±12	-120±12	-122±15

a χ: purine $O_{4'}$-$C_{1'}$-N_9-C_4 torsional angle, pyrimidine $O_{4'}$-$C_{1'}$-N_1-C_2 torsional angle

DISCUSSION

The dNTP Binding Site. The binding of a ligand to a macromolecule can often be qualitatively and quantitatively described from changes in ^{1}H-relaxation rates. In the case of the nucleotide-RT complexes, the change in ligand relaxation rate is apparent from increases in the $\Delta\nu_{obs}$ values of ligand resonances in the presence of protein. The nOe studies indicate line broadening is not only a result of a change in τ_c upon binding to the protein but also due to the inclusion of new magnetic neighbors in the cross-relaxation pathway of the ligand. The concentration- dependent changes of ligand $\Delta\nu_{obs}$ values in the presence of RT and the negative nOes indicate the ligand is in fast exchange on the NMR time scale. As a consequence, equation 1 can be used to calculate the apparent K_d values for the binding of dNTPs to the enzyme. Utilizing the K_d for the dTTP-RT complex of 7.92±1.06 x 10^{-5} M calculated with equation 1, and assuming the on-rate of dTTP to the enzyme is diffusion controlled (approximately 10^8 to 10^7 $M^{-1}s^{-1}$) [35,36], the calculated off-rate is between 6.7 x 10^2 and 8.9 x 10^3 sec^{-1}, which is in the fast exchange region on the NMR time scale.

The magnitude of the K_d value for dTTP binding is comparable to that reported in fluorescence binding studies of the protein [14]. The Hill coefficient of 1 indicates the order of the binding reaction with respect to the concentration of dTTP to be 1, i.e. there is a single binding site for the ligand on the heterodimeric enzyme. Thus, even at the relatively high

protein concentrations required to carry out the NMR experiments (76μM), the magnitude and specificity of nucleotide binding is similar to that reported in fluorescence binding and kinetic studies [14].

Competitive binding studies carried out using the six unique combinations of the four natural dNTPs and dTTP versus AZTTP have shown initial binding to be mutually exclusive in each case [14]. This may be the result of the different dNTPs occupying the same initial binding site, or binding to spatially unique but coupled sites. The nOe experiments can be used to distinguish between these two possibilities by identifying amino acid residues common to the binding site of each ligand. Similar nOe patterns observed for different ligands provide evidence for common contact points on the protein. Examination of the data in Table 1 indicates transferred nOes common to dATP, dTTP, and AZTTP are observed in the aliphatic region of the spectrum upon irradiation at 0.58± 0.02, 0.79 ± 0.02, and 1.26 ± 0.02 ppm. A common pattern of transferred nOes from the aromatic region of the spectrum at 6.73 ± 0.2 ppm is observed to the H1', H2" and the aromatic resonances of dATP and dTTP but not AZTTP. Thus, it appears that while the binding sites of these ligands share common contact points, they are not totally coincident. The 3'-azido group changes the orientation of AZTTP on the protein surface relative to the parent compound dTTP. Perhaps it is this change in orientation that allows site mutations to occur that affect AZTTP but not dTTP binding [38,39]. In a similar transferred nOe study of dATP and dTTP with the Klenow fragment of *E. coli* DNA polymerase I, dATP and dTTP were found to have overlapping binding sites [11].

Although an unambiguous assignment of the protein ^{1}H resonances yielding the transferred nOes is difficult based on chemical shift alone, the positions of these resonances can provide some insight into the types of amino acid residues proximal to the ligand. The magnitude of the nOes to the H2' and H2" resonances of the 2'-deoxyribose ring of dATP in the dATP-RT complex produced upon irradiation at 6.73 and 7.0 ppm suggests the proximity of the C2 methylene to an aromatic residue with an AB spin system (Tyr, Trp, or Phe). The nOes to Hl' and H2'/H2" in the dTTP-RT complex are observed upon irradiation at 7.0 ppm but not at 6.73 ppm. This result can be attributed to the proximity of a different aromatic residue, or to a reorientation with respect to the position of the aromatic residue assigned above. Nucleotide nOes observed upon irradiation of the aliphatic resonances between 0.6 and 1.6 ppm demonstrate the proximity of the nucleotides to hydrophobic protein residues. The nOes arising from irradiation between the 0.6 and 1.0 ppm region can be tentatively attributed to Val, Ile, Met and/or Leu, and between the 1.44 to 1.65 ppm region to the gamma methylene resonances of Lys. Although there is no direct proof, examination of the primary

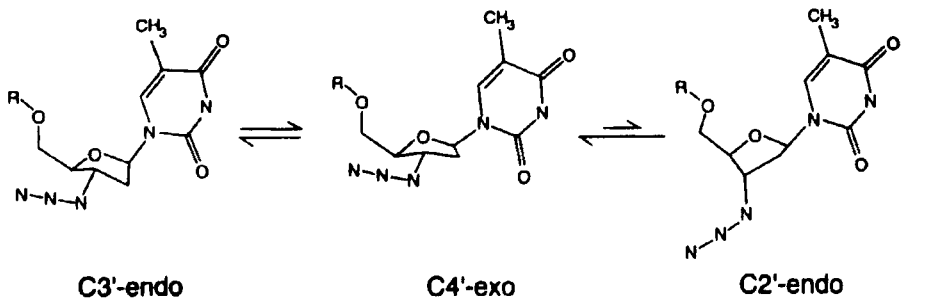

5. Structures of anti dAZT illustrating the 2', 3'-deoxyribose conformational equilibria along the pseudorotational pathway from C3'-endo to C2'-endo.

sequence of HIV-1 RT in the region of the dTTP cross-linking site at Lys-73 [37] suggests likely candidates for the above residues are Lys-65, Lys-66, Lys-70, Lys-73, Leu-74, and Val-75. Further evidence for the involvement of Lys-70, Lys-73 or Leu-74 in nucleotide recognition and initial binding is provided by site-directed mutagenesis studies at Asp-67 and Lys-70 [38], and Leu-74 [39].

Conformation of Bound Nucleotide. The conformation of protein-bound ligands can be obtained with the use of TOE experiments [20]. Interproton distance ratios were calculated either from the cross-relaxation rates determined from the initial slope of TOE buildup curves or from pre-steady state TOEs. The experimentally determined interproton distance ratios were then compared to theoretical values derived from models to obtain the bound-ligand conformation. The lack of a 2'-deoxyribose Hl' to pyrimidine H6 or 2'-deoxyribose Hl' to purine H8 nOe indicated the bound ligands are exclusively in the anti conformation. This is in contrast to free solution, where both dTTP and AZTTP are in a syn-anti equilibrium [29]. Based on the models utilized here, the ring pucker observed for all protein-bound nucleotides examined is predominantly C4'-exo with partial C3'-endo character. It should be noted that this might be the time-averaged conformation as illustrated in Figure 5. If the rate of pseudorotation of the deoxyribose ring in the bound state is fast compared to the off rate, the conformational equilibrium may have shifted from the 1/1 C3'-endo/C2'-endo composition reported in solution [29] toward the C3'-endo state (1.4/1.0 C3'-endo/C2'-endo). Alternatively, the ring pucker of the bound-ligand may exist in two or more conformations and the averaged nOe was observed. The nOe ratios of H6-H5"/H6-H3' for dTTP and AZTTP are consistent with a +synclinal $C_{4'}$-$C_{5'}$ torsion angle for dTTP and AZTTP. The conformation of AZTTP reported here corresponds to the conformation of AZTTP observed by Huang et al. [10] in the active site.

REFERENCES

1. Hoffman A.D., Banapour B. and Levy J.A. **1985** Virology 147, 326-335.

2. DiMarzo, V.F., Copeland, T.D., DeVico, A.L., Rahman, R., Orozlan, S., Gallo, R.C. and Sarngadharan, M.G. **1986** Science 231, 1289-1291.

3. Johnson, M.S., McClure, M.A., Feng, D. –F., Gray J. and Doolittle R.F. **1986** Proc. Natl. Acad. Sci. U.S.A. 83, 7648-7652.

4. Hansen J., Schulze T., Mellert W. and Moelling K. **1988** EMBO J. 7, 239-243.

5. Majumdar C., Abbotts J., Broder S. and Wilson S.H. **1988** J. Biol. Chem. 263, 15657-15665.

6. Bryant F.R., Johnson K.A. and Benkovic S.J. **1983** Biochemistry 22, 3537-3546

7. Hopkins S., Furman P.A. and Painter G.R. **1989** Biochem. Biophys. Res. Commun. 163, 106-110.

8. Kohlstaedt L.A., Wang J., Friedman J.M., Rice P.A. and Steitz T.A. **1992** Science 256, 1783-1790.

9. Arnold E., Jacobs-Molino A., Nann R.G., Williams R.L., Lu X., Ding J., Clark Jr, A.D., Zhang, A., Ferris A.L., Clark P., Hizi A. and Hughes S.H. **1992** Nature 367, 85-89.

10. Huang H., Chopra R., Verdine G.L. and Harrison, S.C. **1998** Science 282, 1669-1675.

11. Ferrin L.J. and Mildvan A.S. **1985** Biochemistry 24, 6904-6913.

12. Tisdale M., Ertl P., Larder B.A., Purifoy D.J., Darby G. and Powell K.L. **1988** J. Virol. 62, 3662-3667

13. Altman S. and Lerman L.S. **1970** J. Mol. Biol. 50, 235-261.

14. Painter G.R., Wright L.L., Hopkins S. and Furman P.A. **1991** J. Biol. Chem. 266, 19362-19368.

15. Brewer J.M., Pesce A.J. and Ashworth R.B. **1974** Experimental Techniques in Biochemistry, Prentice-Hall, Englewood Cliffs, p. 364.

16. Gibbons W.A., Beyer C.F., Dadok J., Sprecher R.F. and Wyssbrod H.R **1975** Biochemistry 14, 420-429.

17. Glasel J.A. **1989** J. Mol. Biol. 209, 747-761.

18. James T.L. **1975** Nuclear Magnetic Resonance in Biochemistry: Principles and Applications pp. 59-60, Academic Press, New York.

19. Fersht A.R. **1985** Enzyme Structure and Mechanism, 2nd ed. pp 272-273, W.H. Freeman and Co., New York.

20. Olejniczak E.T., Poulsen F.M. and Dobson C.M. **1981** J. Am. Chem. Soc. 103, 6574-6580.

21. Dobson C.M., Olejniczak ET., Poulsen F.M. and Ratcliffe R.G. **1982** J. Magn. Reson. 48, 97-110.

22. Clore, G.M. and Gronenborn, A.M. **1982** J. Magn. Reson. 48, 402-417.

23. Clore G.M. and Gronenborn A.M. **1983** J. Magn. Reson. 53, 423-442.

24. Noggle J.H. and Schirmer R.E. **1971**. The Nuclear Overhauser Effect: Chemical Applications pp. 45-50, Academic Press, New York.

25. Mohamadi F., Richards N.G.J., Guida W.C., Liskcamp R., Lipton M., Caulfield C., Chang G., Hendrickson T. and Still W.C. **1990** J. Comp. Chem. 11, 440-467.

26. Weiner S.J., Kollman P.A., Nguyen D.T. and Case D.A. **1986** J. Comput. Chem. 7, 230-252.

27. Painter G.R., Shockcor J.P. and Andrews C.W. **1990** Adv. Mol. Model. 2, 135-163.

28. Birnbaum, G.I., Giziewicz, J., Gabe, E.J., Lin, T.-S. and Prussoff, W.H. **1987** Can. J. Chem. 65, 2135-2139.

29. Singh U.C. and Kollman P.A. **1984** J. Comput. Chem. 5, 129-145.

30. Herzyk P., Beveridge A. and Neidle S. **1987** Biochem. Biophys. Res. Commun. 145, 1356-1361.

31. Hassnoot A. **1992** J. Amer. Chem. Soc. 114, 882-888.

32. Fry D., Cook C., Pritcher R., Greeley D., Huryn D., Holman M., Gruninger-Leitch F. and Sim I. **1990** FASEB J. 4, A1841.

33. Plochocka A., Rabczenko A. and Davis D.B. **1981** J. Chem. Soc. Perkin H, 82-89.

34. Saenger, W. **1984** Principles of Nucleic Acid Structure, pp. 79-82, Springer-Verlag, New York.

35. Hammes G.G. and Schimmel P.R **1970** The Enzymes, 3rd Ed. 2, 67-114.

36. Fersht A.R. **1985** Enzyme Structure and Mechanism, 2nd ed. pp 150-151, W.H. Freeman and Co., New York.

37. Cheng N., Painter G.R. and Furman P.A. **1991** Biochem. Biophys. Res. Commun. 174, 785-789.

38. Larder B.A. and Kemp S.D. **1989** Science 246, 1155-1158.

39. St. Clair M.H., Martin J.L., Tudor-Williams G., Bach M.C., Vavro C.L., King D.M., Kellam P., Kemp S.D. and Larder B.A. **1991** Science 253, 1557-1559.